

# *Progress in Phosphorescence Lifetime Measurement Instrumentation for Oxygen Sensing*

ANGEL DE LA TORRE-VEGA<sup>\*a</sup>, SANTIAGO  
MEDINA-RODRÍGUEZ<sup>b</sup>, CARLOS MEDINA-RODRÍGUEZ<sup>b</sup> AND  
JORGE F. FERNÁNDEZ-SÁNCHEZ<sup>c</sup>

<sup>a</sup>Department of Signal Theory, Telematics and Communications, University of Granada, 18071, Granada, Spain; <sup>b</sup>MODOTIC S.L., C/ Jardines 7, 18195, Cúllar Vega (Granada), Spain; <sup>c</sup>Department of Analytical Chemistry, University of Granada, 18071, Granada, Spain

\*E-mail: atv@ugr.es

## **6.1 Introduction**

The phosphorescence of a sensing phase is associated to the radiative deactivation of excited states in a phosphorescent material. In oxygen sensitive materials, the phosphorescence is altered by the presence of oxygen because the oxygen provides non-radiative deactivation mechanisms from the excited to the fundamental states. The non-radiative deactivation quenches the phosphorescence and reduces both the luminescent intensity and the luminescence lifetime. Since the magnitude of the quenching is a function of the

oxygen concentration, an appropriate measurement of the phosphorescence intensity and/or lifetime, together with an appropriate calibration, is the principle of phosphorescence instrumentation for oxygen sensing.<sup>1-4</sup>

The phosphorescent sensing phase can be considered as a linear system, excited with a light source and generating a phosphorescence response according to its corresponding linear differential equation. The relationship between the input and the output of the sensing phase can be equivalently described with the linear differential equation (*i.e.* the coefficients of the equation), its impulsive response (*i.e.* the phosphorescence response to an impulsive excitation) or its frequency response (*i.e.* the attenuation and the phase-shift of the response when it is excited with a sinusoidally modulated source). As in any linear system, the frequency response  $H(j\omega)$  is the Fourier's transform of the impulsive response  $h(t)$  (where  $\omega = 2\pi f$  is the angular frequency in radians/s and  $j$  is the imaginary unit of complex numbers), and the emission response  $x_{em}(t)$  to an arbitrary excitation  $x_{exc}(t)$  can be calculated either in the time domain as the convolution of the excitation and the impulsive response,  $x_{em}(t) = x_{exc}(t) * h(t)$ , or in the frequency domain as the product of the Fourier's transform of the excitation signal with the frequency response,  $X_{em}(j\omega) = X_{exc}(j\omega) \cdot H(j\omega)$ .<sup>5,6</sup>

The simplest model for describing phosphorescent sensing phases is a first order differential equation, with a time constant (or lifetime) as unique relevant coefficient, which is a function of the analyte concentration. The solution of this equation describing the phosphorescence when the system is excited with a pulsed light is a mono-exponential decay characterized by the lifetime constant, while the frequency response is a first order low-pass filter with a cut-off frequency inversely proportional to the lifetime.<sup>7</sup> The change of the lifetime with the quencher concentration is reasonably described by the Stern–Volmer equation as a first approach.<sup>1,8</sup> Even though the Stern–Volmer equation and the first order differential equation qualitatively describe a wide range of sensing phases (and also provide accurate modelling for some of them), a higher order differential equation and a more complex description of the quenching effect are necessary to provide an accurate description of many sensing phases.<sup>9</sup>

From the point of view of instrumentation for oxygen sensing, the phosphorescence lifetime can be determined in the time domain or in the frequency domain. In the first case, a pulsed illumination source is required and the oxygen determination is obtained by analyzing the evolution in time of the phosphorescence response (which is approximately a mono-exponential decay). The frequency domain measurements require a modulated illumination source and the analysis of the amplitude and/or phase of the phosphorescence response relative to those of the excitation signal (which approximately correspond to a first order low-pass filter). Even though both are mathematically equivalent, there are some differences to be considered for designing a phosphorescence instrument:

- Usually the phosphorescent system is not a first order model (*i.e.* the mono-exponential decay or the first order low-pass filter are not accurate enough). In this case a lifetime constant is not well defined, and in

time domain measurements, the observed lifetime depends on the time interval used for measuring it.<sup>1,4</sup>

- The measurements are always affected by background noise due to the noise generated by the optoelectronic devices, amplifiers and background illumination. Additionally, the signal-to-noise ratio (SNR) is particularly low in some applications, such as in the case of small samples (due to the small amount of light emitted by the sensing phase).<sup>10,11</sup> Dealing with noise (and therefore optimizing the accuracy in the measurements) is significantly easier in the frequency domain than in the time domain.<sup>12,13</sup>
- Time domain measurements are based on pulsed illumination sources and require expensive and complex instrumentation using high-speed photodetectors.<sup>1</sup> On the other hand, frequency domain lifetime determination can be implemented with cheaper light sources and electronic components.<sup>14,15</sup>

In recent years, optoelectronic devices appropriate for frequency domain measurements (LEDs for medium power at short wavelengths, photodiodes, preamplified photodiodes, phototransistors, *etc.*) have become cheaper. Additionally, small computers (Raspberry-Pi) and microcontrollers have improved their capabilities (in terms of available memory, computational efficiency, velocity, analog-to-digital (AD) and digital-to-analog (DA) conversion, interconnectivity with other systems, power consumption, *etc.*) at a reasonable cost. These components and devices provide a new context in which flexible and non-expensive phosphorescence instruments based on frequency domain measurements can be designed.<sup>16–20</sup> A modular architecture like that proposed in ref. 21, 22 considers the phosphorescent system as a linear system, modelled with a linear differential equation (or a frequency response), which is excited with a modulated light source and responds with a phosphorescence recorded by a photodetector device. A computer or a microcontroller can be used to prepare a digital signal to modulate the illumination source (the digital signal is DA-converted and amplified to excite a LED source). The electrical signal provided by the photodetector can be amplified and AD-converted, and the digital signal can be processed by a microcontroller or a computer.

Under this perspective, the flexibility for exciting the sensing phase and processing the phosphorescence response can be exploited in order to optimize the information provided by the phosphorescence instrument. Several obvious advantages are derived from the proposed architecture. Since both the excitation and the recorded signals are digital, signal processing can be performed with numerical algorithms programmed in a microcontroller or a computer, and the complexity of the algorithms is not a strong limitation in the design of the phosphorescence instrument. Since the phosphorescent system is assumed to be linear, all the signal theory related to linear systems (and commonly applied in modern communication systems) can be applied and exploited.<sup>5,7</sup> And finally, since the configuration of the measuring procedure requires just programming an algorithm, the design of the instrument

can be easily adapted to specific requirements or measuring scenarios in order to optimize the information provided by the sensing phase. In this chapter we describe how signal processing applied to instruments based on this architecture can be exploited to provide an optimal characterization of the sensing phase, to improve the accuracy of the oxygen determination, to provide a confidence interval of the oxygen determination (based on the estimated background noise), or to optimally integrate information from several harmonics in a single accurate oxygen determination.

## 6.2 The Phosphorescence Emission as a Linear System

This section describes the fundamental equations of a phosphorescent system, and how it can be considered as a linear system described by its corresponding differential equation or its frequency response.

### 6.2.1 First Order Phosphorescent Systems

In the simplest phosphorescence model, the population of the excited state  $N(t)$  increases linearly with the illumination  $x_{\text{exc}}(t)$  and decreases linearly with the population according to the constants  $\Gamma_r$  and  $\Gamma_{\text{nr}}$  describing, respectively, the radiative and the non-radiative decays from the excited to the fundamental states:

$$\frac{dN(t)}{dt} = a_0 x_{\text{exc}}(t) - (\Gamma_r + \Gamma_{\text{nr}})N(t) \quad (6.1)$$

where  $a_0$  is a constant that relates the illumination used as excitation with the increase of the excited state population in the phosphorescent material. This first order linear differential equation is characterized by a time constant or lifetime that is inversely proportional to the sum of the decay constants. The simplest quenching model considers that the non-radiative decay constant increases linearly with the quencher concentration  $C$  and, in this case, the dependence of the lifetime with  $C$  is described by the Stern–Volmer equation:

$$\tau_q = \frac{1}{\Gamma_r + \Gamma_{\text{nr}}} = \frac{1/\Gamma_r}{1 + \Gamma_{\text{nr}}/\Gamma_r} = \frac{\tau_0}{1 + kC} \quad (6.2)$$

where  $k$  is the Stern–Volmer constant and  $\tau_0$  is the lifetime in absence of quencher.<sup>1,8</sup>

The phosphorescence emission  $x_{\text{em}}(t)$  is proportional to the radiative decay ( $\Gamma_r N(t)$ ) and, therefore, the phosphorescence can be described with a similar differential equation:

$$\frac{dx_{\text{em}}(t)}{dt} = a_1 x_{\text{exc}}(t) - \frac{x_{\text{em}}(t)}{\tau_q} \quad (6.3)$$

where  $a_1$  is a constant that relates excitation with emission. This equation can be rewritten in the Fourier domain:<sup>6</sup>

$$j\omega\tau_q X_{em}(j\omega) = \tau_q a_1 X_{exc}(j\omega) - X_{em}(j\omega) \quad (6.4)$$

where the derivative operator has been transformed into  $j\omega$  and  $X_e(j\omega)$  is the Fourier transform of  $x_e(t)$  (for both the excitation or the emission signals). The frequency response of the phosphorescent system is therefore:

$$H(j\omega) = \frac{X_{em}(j\omega)}{X_{exc}(j\omega)} = \frac{\tau_q a_1}{1 + j\omega\tau_q} \quad (6.5)$$

or equivalently, using frequency instead of angular frequency:

$$H(C, f) = M_0 \frac{\tau_q}{\tau_0} \frac{1}{1 + j2\pi f\tau_q} \quad (6.6)$$

where  $M_0$  is the modulation-factor (ratio between emission and excitation) at null quencher concentration and low frequencies, and the dependence of the lifetime with the quencher concentration is given by eqn (6.2). This equation describes that an increment of the quencher concentration reduces both the lifetime and the luminescence intensity. Additionally, the frequency response of the phosphorescent system is a low-pass filter with a cut-off frequency that increases with the quencher concentration.

The frequency response is a complex function, *i.e.*, it contains real and imaginary parts, or, equivalently, magnitude and phase. The magnitude or modulation-factor describes the ratio between the amplitudes of the emission and the excitation when the phosphorescent system is excited with a sinusoidally modulated illumination:<sup>1</sup>

$$m(C, f) = \sqrt{|H(C, f)|^2} = M_0 \frac{\tau_q}{\tau_0} \frac{1}{\sqrt{1 + (2\pi f\tau_q)^2}} \quad (6.7)$$

and the phase-shift represents the delay between both sinusoidal waves:<sup>1</sup>

$$\phi(C, f) = -\arctan(2\pi f\tau_q) \quad (6.8)$$

## 6.2.2 Multi-exponential Phosphorescent Systems

A usual model for describing higher order phosphorescent systems includes several phosphorescence processes. This multi-site phosphorescence model is described by a frequency response including the additive contribution of each individual process:

$$H(C, f) = M_{01} \frac{\tau_{q1}}{\tau_{01}} \frac{1}{1 + j2\pi f\tau_{q1}} + M_{02} \frac{\tau_{q2}}{\tau_{02}} \frac{1}{1 + j2\pi f\tau_{q2}} + \dots \quad (6.9)$$

where  $M_{0i}$ ,  $\tau_{0i}$  and  $\tau_{qi}$  are associated with the  $i$ th process and  $\tau_{qi}$  describes the reduction of the  $i$ th lifetime according to a Stern–Volmer constant  $k_i$ . The frequency response is again a complex function with real and imaginary parts, or with magnitude and phase describing the modulation-factor and the phase-shift of the emission with respect to the excitation signals, for each frequency component  $f$ .

The time domain version of the multi-site model is an impulsive response (obtained as the inverse Fourier transform of the frequency response) consisting of a multi-exponential decay (additive contribution of several exponential processes), dominated by the shortest lifetimes for the early part of the decay and by the longest lifetimes for the late part of the decay. Obviously, there is a lifetime  $\tau_{qi}$  defined for each subprocess but the global process cannot be described as a mono-exponential decay. For this reason, the estimation of  $\tau_q$  in a multi-exponential system is an apparent lifetime (rather than a proper lifetime) whose value depends on the procedure defined for measuring it.<sup>1</sup>

### 6.2.3 Lifetime Derived from Modulation Factor and Phase-shift

From eqn (6.7) and (6.8), modulation-factor and phase-shift based lifetimes can be derived for mono-exponential phosphorescent systems:<sup>2</sup>

$$\tau_\phi(f) = \frac{-\tan(\phi(f))}{2\pi f} \quad (6.10)$$

$$\tau_m(f) = \tau_0 \frac{m(f)/m_0(f)}{\sqrt{1 + (2\pi f \tau_0)^2 (1 - (m(f)/m_0(f))^2)}} \quad (6.11)$$

where  $m_0(f)$  is the modulation-factor at frequency  $f$  and at null quencher concentration<sup>†</sup>. Both lifetime estimations should be equal in mono-exponential systems, but they should be considered apparent lifetimes in a general phosphorescent system and both estimations are not expected to be equal. Similarly, the estimated lifetimes at different modulation frequencies should be identical in a mono-exponential system, but apparent lifetimes could change with the frequency in a general phosphorescent system.<sup>1</sup> From the instrumentation point of view, phase-shift lifetime estimations are usually preferred to those based on modulation-factors because the degradation of the phosphorescent material<sup>23</sup> or sub-optimal optical

---

<sup>†</sup>Note that for low modulation frequencies (*i.e.* much smaller than the cut-off frequency)

$\tau_m(f) \approx \tau_0 \frac{m(f)}{m_0(f)} \approx \tau_0 \frac{I}{I_0}$ , and the modulation-factor based lifetime can be estimated with

the phosphorescence intensity relative to that at null quencher concentration.

coupling (when some optical element is replaced) reduces the constant  $m_0(f)$  and an accurate determination of  $\tau_m(f)$  usually requires a frequent recalibration of  $m_0(f)$ .

### 6.2.4 Modelling and Calibration of Phosphorescent Systems

Assuming that the phosphorescent system is linear, the description of the phosphorescence at a given quencher concentration is provided by the frequency response, and therefore a complete description of the phosphorescence requires the estimation of the frequency response at different quencher concentrations. A consistent description of the phosphorescence, appropriate for multi-frequency measurements, should avoid the use of apparent lifetimes and would fit the multi-exponential frequency response proposed in eqn (6.9) for different frequencies and quencher concentrations.

Since many phosphorescence instruments work at a single frequency, an alternative description consists of the estimation of the apparent lifetime (either modulation-factor or phase-shift based) at the selected modulation frequency as a function of the quencher concentration.<sup>2,23-25</sup> Usually, the Demas model (derived from the multi-exponential model) is applied to describe the dependence of the apparent lifetime with the quencher concentration:<sup>1,26</sup>

$$\tau(C, f) = \tau_0(f) \left( \frac{x_1(f)}{1 + k_1(f)C} + \frac{x_2(f)}{1 + k_2(f)C} + \dots \right) \quad (6.12)$$

where the dependence with the frequency is indicated to remark that the Stern–Volmer constants  $k_i$ , the apparent lifetimes (at null and at  $C$  concentrations) and the constants  $x_i$  can change with the frequency due to the inconsistency inherent to the use of apparent lifetimes.

For modelling purposes, a global modelling using eqn (6.9) (providing consistent information about individual subprocesses) is preferable. For oxygen determination purposes, the Demas model applied at each individual frequency to each apparent lifetime provides more flexibility in the modelling (more constants to be fitted) and a more accurate determination of the oxygen concentration can be obtained if the measuring instrument is appropriately calibrated.<sup>2,9</sup>

## 6.3 Architecture for Measuring the Frequency Response

As previously discussed, a phosphorescent system appropriate for oxygen determination can be modeled as a linear system characterized by its frequency response (which significantly changes according to the oxygen concentration). A first order model (given by eqn (6.6) and (6.2)) qualitatively describes most phosphorescent systems, even though an accurate enough description requires the multi-exponential model in eqn (6.9). In any case,

the phosphorescence instrumentation for oxygen determination can be conceived as an instrument for estimating the frequency response (*i.e.* the modulation-factor and the phase-shift) at one or several modulation frequencies, and more specifically, to accurately measure the changes in the frequency response associated to variations in the oxygen concentration.

### 6.3.1 Modular Architecture of the Phosphorescence Instrument

Medina *et al.* have proposed a modular architecture for measuring the frequency response of the phosphorescent system.<sup>2,21,27,28</sup> As described in Figure 6.1, a central system (a computer or a microcontroller) configures the signal to be used as excitation (a digital signal at a sampling frequency, with a specific duration, containing one or several frequency components). This signal is digital-to-analog converted and amplified in order to provide a modulated illumination with a LED at the excitation wavelength. The sensing phase, excited by the LED illumination, generates a phosphorescence response at the emitting wavelength conditioned by its frequency response. The phosphorescence response is converted into an electrical signal by the photodetector. This signal is amplified and analog-to-digital converted. Both the excitation and the emission digital signals are then processed by the central system in order to estimate the frequency response (modulation-factor and phase-shift) of the sensing phase at the modulation frequency (or at several modulation frequencies if the excitation signal contains several frequency components). This frequency response is used either for the characterization of the sensing phase or for the determination of the oxygen concentration (after appropriate calibration).

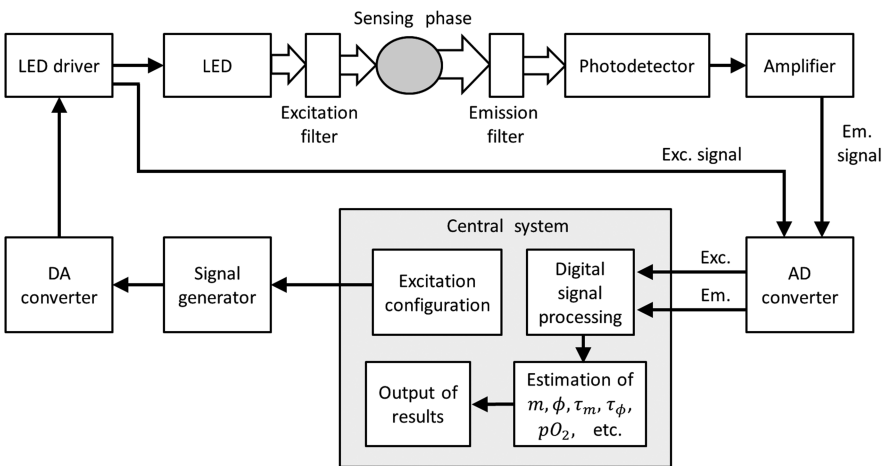


**Figure 6.1** Architecture of the phosphorescence instrument for estimating the frequency response.

This modular architecture allows an easy adaptation to specific requirements. For example, the excitation can be prepared with a computer and a DA board (for an easier and faster configuration) or with a microcontroller (for a cheaper and more portable instrument). The modulation frequency, amplitude and duration of the excitation signal can be programmed (in order to acquire faster measurements or more accurate measurements). The LED driver and the LED can be chosen in order to accommodate the illumination power and excitation wavelength requirements. Similarly, the photodetector and its amplifier can be chosen in order to accommodate the emission wavelength, the phosphorescence intensity and the detector sensitivity. The phosphorescence response can be recorded with a digital oscilloscope, with an AD board or with a microcontroller (with the corresponding implications regarding costs and flexibility). A two-channel AD converter is recommendable to simultaneously record both the excitation and the emission signals, in order to guarantee synchronization between both signals and accurately measure the phase-shift. Digital signal processing of the samples as well as the calibration and determination of the oxygen concentration can be performed with a microcontroller or with a computer.

### 6.3.2 Estimation of the Frequency Response

In order to estimate the frequency response of the phosphorescent system at a given modulation frequency  $f_m$ , the excitation signal should contain a component of this frequency. The emission signal will then contain a component of this modulation frequency. The digital versions of the excitation and emission signals, digitized at a sampling frequency  $f_s$ , are:

$$x_e[l] = A_e \cos(2\pi f_m l / f_s + \phi_e) + N_e[l] \quad (6.13)$$

where  $l$  is the sample index, subindex  $e$  stands for excitation or emission signals,  $A_e$  and  $\phi_e$  are the amplitude and phase of the signals, and  $N_e[l]$  is the noise affecting the signals (including the DC<sup>‡</sup> component, other frequency components and random noise). The correlation of the input signal with a pair of sinusoidal signals in quadrature (a cosine and a sine of frequency  $f_m$ ) provide the in-phase and the quadrature components:<sup>2,7</sup>

$$I_e(f_m) = \frac{1}{K} \sum_l x_e[l] \cos(2\pi f_m l / f_s) \quad (6.14)$$

$$Q_e(f_m) = \frac{1}{K} \sum_l x_e[l] \sin(2\pi f_m l / f_s) \quad (6.15)$$

---

<sup>‡</sup>DC (from "Direct Current"): level of continuous signal or, equivalently, component at null frequency.

where  $K$  is a normalization constant. The I/Q components provide an estimation of the amplitude and phase of the  $f_m$  component of  $x_e[l]$ :

$$A_e(f_m) = \sqrt{I_e^2(f_m) + Q_e^2(f_m)} \quad (6.16)$$

$$\phi_e(f_m) = -\arctan(Q_e(f_m)/I_e(f_m)) \quad (6.17)$$

and from the amplitude and phase of the excitation and emission signals, the modulation-factor and the phase-shift of the frequency response can be estimated at the frequency  $f_m$ :

$$m(f_m) = A_{em}(f_m)/A_{exc}(f_m) \quad \phi(f_m) = \phi_{em}(f_m) - \phi_{exc}(f_m) \quad (6.18)$$

This procedure, known as In-phase/Quadrature estimation (or I/Q),<sup>2,7</sup> is also the principle of lock-in amplifiers (LIA)<sup>29,30</sup> commonly used in phosphorescence instrumentation. From a reference input (usually the excitation signal), the LIA instrument generates a pair of sinusoidal signals in quadrature (a cosine wave, in phase with the reference signal, and a sine wave, in quadrature with it). Both signals are multiplied with the signals to be analyzed ( $x_{exc}(t)$  and  $x_{em}(t)$ ) and the resulting signals are then low-pass filtered to obtain the in-phase and the quadrature components for each signal. They are then used to estimate the amplitudes and phases of the input signals, and to estimate the modulation-factor and the phase-shift at the modulation frequency.

I/Q detection is optimal in the sense that the noise minimally affects the estimations at the modulation frequency (the estimations are affected only by the component of the noise at the frequency  $f_m$ ). Even though the measurement principles used in I/Q and LIA are very similar, there are some practical details to take into consideration. LIA instruments work at a single frequency, while I/Q method can independently be applied to each frequency component of a signal containing several harmonics. Additionally, LIA instruments include predefined low-pass filters (to select configurable measuring times) and the estimations of the in-phase and quadrature components are affected by the impulsive response of the selected low-pass filter. I/Q and LIA based instruments have been compared in ref. 27 at different SNR conditions and using both, synthetic signals and signals recorded from a phosphorescent system for measuring the oxygen concentration. Performances for both instruments are similar even though I/Q provides slightly better accuracy (mainly due to the restriction of the low-pass filters in the LIA instruments) and more flexibility in the configuration of the measuring process.

The modulation-factor and the phase-shift can be also estimated from the Fast Fourier Transform (FFT) of the excitation and emission signals.<sup>13,31</sup> The in-phase and quadrature components for the modulation frequency  $f_m$  are equivalently estimated as the real and imaginary parts of the FFT component corresponding to  $f_m$ . This requires that all the energy of the modulation frequency is concentrated in just one frequency

component of the FFT. This condition is verified if the duration of the signal to be processed contains an integer number of cycles at the modulation frequency. While using the I/Q method with pre-stored cosine and sine waves is more efficient for single-frequency estimations or multi-frequency estimations with few frequency components, the FFT method is computationally more efficient when the excitation signal contains more frequency components.

## 6.4 Multifrequency Measurements and Applications

The proposed architecture of the phosphorescence instrument allows the use of multi-frequency signals.<sup>2,21,31</sup> The excitation signal can be designed to contain several frequency components and independent modulation-factors and phase-shifts can be estimated for each frequency component by applying the I/Q or the FFT based procedures to the  $x_{\text{exc}}[l]$  and  $x_{\text{em}}[l]$  digital signals.

There are several advantages derived from multi-frequency measurements. In the context of the characterization of the phosphorescent system, since it cannot be assumed to be a first order system, an accurate characterization should include the estimation of the frequency response at several modulation frequencies (and, of course, for several quencher concentrations). So, data acquisition using a single-frequency phosphorescence instrument requires repeating the measurements at each single frequency,<sup>23</sup> while a multi-frequency instrument can simultaneously obtain measurements at several modulation frequencies from a single excitation-emission recording.<sup>2,24,25</sup>

In the context of oxygen determination, selecting the optimal modulation frequency for a single-frequency instrument is not trivial: the modulation frequency providing the largest change in the frequency response depends on the quencher concentration. So, a critical decision in the design of a single-frequency phosphorescence instrument is the selection of the modulation frequency, which should be chosen taking into account the sensing phase and the concentration range to be measured.<sup>1,19</sup> The use of multi-frequency measurements allows selecting the optimal modulation frequency at each measuring condition.<sup>21</sup> Finally, since all the modulation frequencies provide information about the oxygen concentration, the determinations provided by each harmonic can be combined in order to obtain a more accurate oxygen determination.<sup>2,31</sup>

Additionally, multi-frequency measurements provide a significantly more efficient management of the illumination intensity. A pure single-frequency modulation is not possible with a light source because sinusoidal signals are negative half of the time (negative illumination is not possible) and light modulation always includes a DC level. This DC level is useless for the frequency response estimation, but increases the power dissipation of the LED (degrading the device and limiting the modulation amplitude) and the photodegradation of the phosphorescent sensing phase. Appropriate design with multi-frequency signals improves the useful/useless ratio of the illumination

intensity.<sup>2,11</sup> A particularly interesting multi-frequency excitation is the short duty-cycle rectangular signal.<sup>2,24,25</sup> It provides sufficient energy at several harmonics with low energy at the DC component. Additionally, rectangular signals are easier (and cheaper) generated since switching electronic components can be used (instead of analog amplifiers).

The next sections describe some applications of the multi-frequency spectroscopy for (a) an accurate characterization of the phosphorescent system, (b) selecting the optimal single modulation frequency and (c) improving the accuracy of the oxygen determination by combining the information provided by the different harmonics.

### 6.4.1 Characterization of the Sensing Phase

The accurate characterization of a sensing phase is an important step in the design of a phosphorescence instrument. The frequency response measured at each oxygen concentration provides information about the concentration range in which the instrument can optimally operate (*i.e.* the range in which a small change in concentration produces a large change in the frequency response) or the optimal modulation frequency (*i.e.* frequency providing the largest measurable change in the modulation-factor or phase-shift). An appropriate characterization also helps to choose the most appropriate sensing phase to determine oxygen under specific conditions.

Conventional single-frequency instruments can be used for the characterization of the sensing phase, but measurements must be repeated for each modulation frequency. In ref. 23, for example, optical sensing nanocomposites are evaluated with single-frequency measurements for selecting the optimal modulation frequency and evaluate the phase-shift changes at different concentration ranges. This characterization required frequency-by-frequency measurements. A similar analysis was performed in ref. 24 (using sensing phases based on copper complexes) but the frequency response was measured with a multi-frequency I/Q scheme. In this case, using 10% duty-cycle rectangular signals, multi-frequency analysis was applied to measure the frequency response simultaneously at several harmonics, with a substantial reduction of the measuring effort. The comparison of the frequency response curves at different oxygen concentrations for two sensing phases presented in ref. 24, clearly shows that one of them is more appropriate for oxygen determination at medium and high concentrations, while the other is better for low and ultra-low concentrations.

The multi-frequency measurements can be also used to fit a global multi-site phosphorescence model of the sensing phase, according to eqn (6.9). In ref. 2, multi-frequency modulation-factor and phase-shift were measured at different oxygen concentrations and a global model was fitted, estimating the constants  $M_{0i}$ ,  $\tau_{0i}$  and  $k_i$  ( $i$  index for each site) by minimizing the mean squared error between the frequency response model and the measurements. Figure 6.2 illustrates the frequency response fitting for a well-known oxygen-sensing film coated at the end of an optical fiber (a Pt(II) porphyrin immobilized in

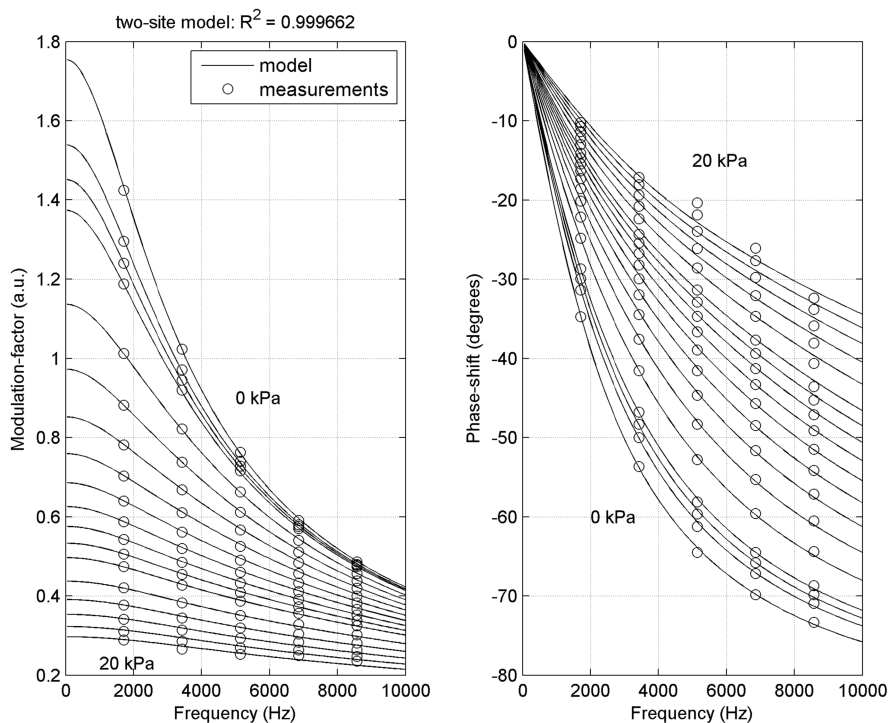


**Figure 6.2** Frequency response of the two-site model (solid lines) fitting the measured modulation-factor and phase-shift (circles). Measurements recorded at concentrations 0, 0.5, 0.75, 1, 2, 3, 4, 5, 6, 7, 8, 9, 10, 12, 14, 16, 18, and 20 kPa O<sub>2</sub>. Model parameters:  $M_{01} = 1.4413$ ;  $k_1 = 0.32278$  kPa<sup>-1</sup>;  $\tau_{01} = 60.31$   $\mu$ s;  $M_{02} = 0.3134$ ;  $k_2 = 0.10108$  kPa<sup>-1</sup>;  $\tau_{02} = 89.60$   $\mu$ s. Adapted with permission from *Anal. Chem.*, 2014, **86**, 5245.<sup>2</sup> Copyright 2014 American Chemical Society.

polystyrene). This figure represents the frequency response measurements (circles) and the frequency response of the model (solid lines) at different concentrations ranging between 0 and 20 kPa O<sub>2</sub>. The measurements were recorded using a 10% duty-cycle rectangular-wave as excitation signal. This fitting corresponds to a two-site model, and the resulting model parameters are indicated in the figure legend. The determination coefficient of the fitting was  $R^2 = 0.999662$ , while it was  $R^2 = 0.995437$  for a one-site (or mono-exponential) model, and  $R^2 = 0.999695$  for a three-site model. These determination coefficients reveal that a one-site model is obviously insufficient for describing the sensing phase ( $R^2$  significantly increases when a two-site model is fitted), and that a three-site model is inappropriate (the number of free parameters increases but it just provides a marginal increase of  $R^2$ ). Therefore, the multi-frequency measurements together with the fitting of the global frequency response provide an appropriate modelling of the sensing phase that is reasonably described, in this case, with a two-site model.

In this example, the residual of the two- and three-site models is associated to noise in the measurements or to the mismatch between the real phosphorescent system and the multi-site model (for this reason no substantial increase of  $R^2$  is observed when modelling with the three-site model). Fitting the measurements at only a single frequency (*i.e.* the third harmonic) increases the determination coefficient to  $R^2 = 0.999905$ , but this model is over-fitted to the measurements at this specific frequency and it is inconsistent when applied to other frequencies. For this reason, when the objective of the phosphorescence instrument is the characterization of the sensing phase, a global multifrequency fitting is preferable (in order to estimate consistent parameters  $M_{0i}$ ,  $\tau_{0i}$  and  $k_i$  valid for most frequencies and concentrations). However, when the phosphorescence instrument is aimed to measure oxygen concentrations at a given range, an individual calibration for each individual frequency is preferable, since it better reduces the residual and provides more accurate oxygen determination, (even though consistency across frequencies of the model parameters is not guaranteed in this case).

#### 6.4.2 Selecting the Optimal Single Modulation Frequency for Analyte Determination

The modulation-factor and the phase-shift are functions of the oxygen concentration and the modulation frequency ( $m = m(C, f)$ ;  $\phi = \phi(C, f)$ ). Conventionally the modulation frequency is considered to be optimal when a small change of the oxygen concentration provides the largest change in the frequency response.<sup>1,19</sup> Mathematically, according to this criterion, the optimal modulation frequency is the one maximizing the partials  $\partial m(C, f)/\partial C$  and  $\partial \phi(C, f)/\partial C$  for modulation-factor and phase-shift based oxygen determinations, respectively. Since the modulation-factor and the phase-shift are functions of both  $C$  and  $f$ , the optimal modulation frequency is expected to depend on the oxygen concentration and is different, in general, for modulation-factor and for phase-shift based oxygen determinations. The multi-frequency characterization of the sensing phase at different oxygen concentrations provides a global model describing  $m(C, f)$  and  $\phi(C, f)$  that can be applied to directly determine the optimal modulation frequency at a given oxygen concentration or for a given range of concentrations. In general, with this criterion, the modulation-factor based determinations are optimal at low modulation frequencies (lower than the cut-off frequency), while the phase-shift based determinations are optimal at a modulation frequency around the cut-off frequency (that strongly depends on the oxygen concentration).<sup>1,4</sup>

However, the previously described procedure does not take into account the effect of the noise in the oxygen determinations. The noise usually modifies the optimal modulation frequency because the phosphorescence intensity decreases with the modulation frequency, and the modulation-factor or phase-shift estimations are more affected by noise at higher modulation

frequencies. In order to take into account the noise, the optimal modulation frequency should be defined as the one minimizing the standard error in the oxygen determination:<sup>2</sup>

$$\text{SE}(C_m) = \left| \frac{\partial C}{\partial m} \right| \text{SE}(m) = \left| \frac{\partial m(C, f)}{\partial C} \right|^{-1} \text{SE}(m) \quad (6.19)$$

$$\text{SE}(C_\phi) = \left| \frac{\partial C}{\partial \phi} \right| \text{SE}(\phi) = \left| \frac{\partial \phi(C, f)}{\partial C} \right|^{-1} \text{SE}(\phi) \quad (6.20)$$

where the standard errors of the modulation-factor and the phase-shift can be estimated from the experimental data (by repeating the measurements), and the partials can directly be obtained from the multifrequency model describing the phosphorescent system.

Medina *et al.*<sup>2</sup> have combined the multi-frequency characterization of the sensing film and the standard errors  $\text{SE}(m)$  and  $\text{SE}(\phi)$  for the estimation of the standard error of the oxygen concentration. This standard error is represented in Figure 6.3 as a function of the modulation frequency, for different oxygen concentrations, and for modulation-factor (left panel) and phase-shift (right panel) based oxygen determinations. In the case of modulation-factor based determinations, the lowest modulation frequency provides the most accurate oxygen determinations. In the case of phase-shift based determinations, there is a well-defined optimal modulation frequency which depends on the oxygen concentration. This dependence with the frequency substantially differs when the effect of the noise is ignored.<sup>2</sup> Usually, under laboratory conditions, the noise can be minimized and appropriately characterized, and for this reason, the determination of the optimal modulation frequency usually ignores the noise when a sensing phase is characterized in laboratory.<sup>24,25</sup> However, when measurements are acquired with portable instruments, the noise conditions could change significantly and therefore the noise should be considered for selecting the optimal modulation frequency.

According to the results in Figure 6.3, taking into account that the oxygen determinations based on the modulation-factor are more accurate than those based on the phase-shift, the former should be preferred for oxygen determination purposes. However, because of the recalibration requirements of modulation-factor based determinations, phase-shift measurements are often preferred.<sup>1,4</sup>

### 6.4.3 Using Multi-frequency Information for Oxygen Determination

Even though the characterization of the phosphorescent system is based on the estimation of the frequency response (either  $H(C, f)$  or equivalently  $m(C, f)$  and  $\phi(C, f)$ ) at different oxygen concentrations, oxygen determination is usually performed with calibration curves describing the changes of

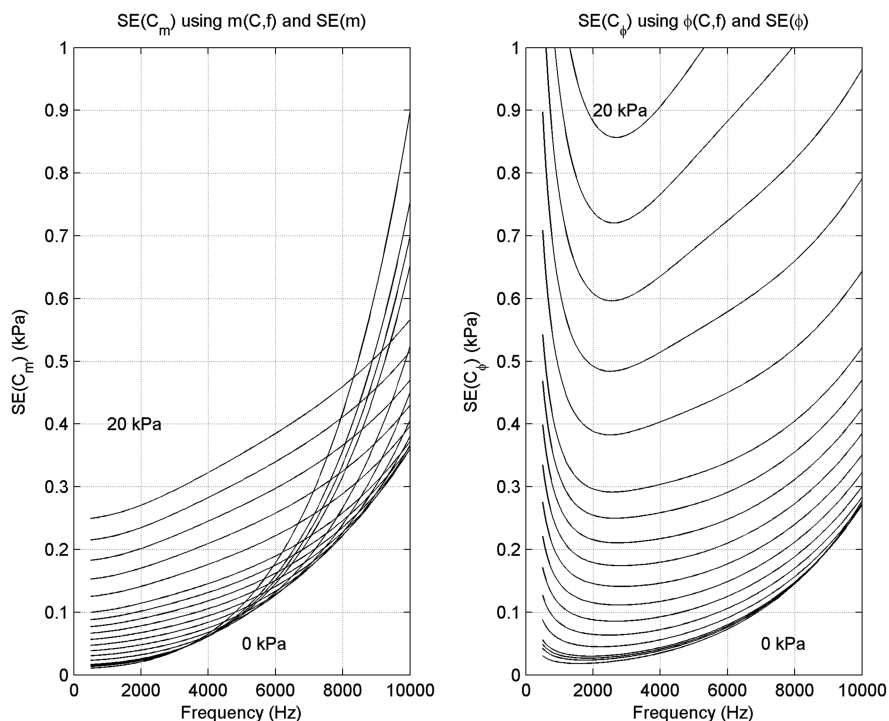


**Figure 6.3** Standard error of oxygen determination,  $SE(pO_2)$ , as a function of modulation frequency when the determination is based on modulation-factor (left panel) or phase-shift (right panel). Curves correspond to the concentrations 0, 0.5, 0.75, 1, 2, 3, 4, 5, 6, 7, 8, 9, 10, 12, 14, 16, 18, and 20 kPa  $O_2$ . The estimation of  $SE(pO_2)$  includes the standard error associated with the measured parameters. Adapted with permission from *Anal. Chem.*, 2014, **86**, 5245.<sup>2</sup> Copyright 2014 American Chemical Society.

the apparent lifetime with the oxygen concentration.<sup>18,26,32–35</sup> The apparent lifetime can be estimated from the phase-shift or from the modulation-factor (eqn (6.10) and (6.11)), at one or at several modulation frequencies. A multi-frequency measuring system allows the simultaneous estimation of the apparent lifetimes ( $\tau_m(f_i)$  and  $\tau_\phi(f_i)$ ) at several modulation frequencies ( $f_i$ ) from a single recording. Due to the inconsistency inherent to the definition of the apparent lifetimes,<sup>2</sup> the limitations of a multi-site model for describing the actual phosphorescent system<sup>35</sup> and in order to optimally fit the experimental data and provide accurate determinations, usually an independent curve is calibrated for each individual apparent lifetime (for each modulation frequency and for both modulation-factor and phase-shift).

Therefore, a multi-frequency phosphorescence instrument appropriately calibrated and using  $I$  modulation frequencies, provides up to  $2I$  independent determinations of the oxygen concentration ( $I$  derived from  $\tau_m(f_i)$  and  $I$  from  $\tau_\phi(f_i)$  obtained from a single signal recording). Medina *et al.*<sup>21</sup> have

compared the accuracy in the oxygen determination for different strategies for combining them: average, weighted average, selecting the optimal determination for each condition (*i.e.* the one closer to the optimal modulation frequency at each measuring condition) or using the estimation corresponding to a globally optimal modulation frequency. They found that a substantial improvement of the instrument accuracy can be achieved, but optimal combination of the independent determinations is not immediate.

A more detailed analysis of the problem showed that the optimal combination of several statistically independent oxygen determinations is a weighted average of the independent determinations with weights inversely proportional to the variance of each one:<sup>2</sup>

$$\hat{C} = \frac{\sum w_i C(\tau_i)}{\sum w_i} \quad w_i = \frac{1}{\sigma_i^2} \quad (6.21)$$

where  $\tau_i$  is an apparent lifetime,  $C(\tau_i)$  is the corresponding calibration curve and  $\sigma_i$  is the standard error associated to the  $i$ th individual determination  $C(\tau_i)$ , which can be estimated according to the error propagation theory using the corresponding calibration curve and the standard error of the lifetime:<sup>2</sup>

$$\sigma_i = \text{SE}(C(\tau_i)) = \left| \frac{\partial C(\tau_i)}{\partial \tau_i} \right| \text{SE}(\tau_i) \quad (6.22)$$

The standard error of the lifetimes can be obtained from several measurements, and can be easily estimated during the instrument calibration. Even though the standard errors should be estimated under the specific noise conditions in which the oxygen is being determined, according to eqn (6.21) the optimal combination remains invariant if the standard errors are all scaled with the same constant. Therefore, if the standard errors are estimated under calibration conditions and these standard errors are applied to measurements at different noise conditions, the main effect of the change in the SNR is a global scaling of the standard errors and the combination proposed in eqn (6.21) would be still valid.

The combination of oxygen determinations based on eqn (6.21) was demonstrated by Medina *et al.*<sup>2</sup> using short duty-cycle rectangular-wave signals as excitation. Figure 6.4 shows root-mean-square error (RMSE) in the oxygen determination at different concentrations, when a conventional sinusoidal signal is used as excitation and when the rectangular signal is used. Results for the rectangular signal including information from 1 to 5 harmonics are shown. Since both excitation signals were configured for the same average intensity, and since the rectangular signal provides more amplitude in the harmonics at the same average intensity, there is a significant improvement for rectangular signals with respect to sinusoidal modulation. This figure also shows that the combination of information from different harmonics decreases the RMSE of the measurements, and the error is smaller as more harmonics are included. The first harmonic of

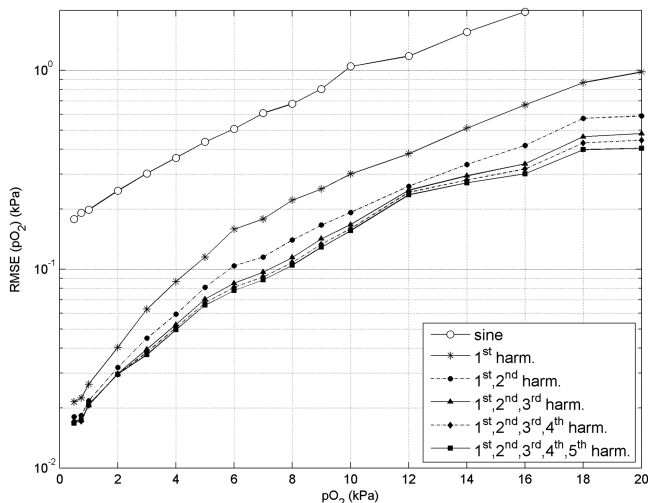


**Figure 6.4** RMSE in determination of  $pO_2$  using single-frequency modulation (sinusoidal) and multi-frequency modulation (rectangular signals). Oxygen determinations based on phase-shift estimations. Determinations with rectangular signals are obtained by combining different harmonics. Adapted with permission from *Anal. Chem.*, 2014, **86**, 5245.<sup>2</sup> Copyright 2014 American Chemical Society.

the rectangular signal achieved an average RMSE 4.4 times smaller than the sinusoidal signal, and the RMSE was 7.4 times smaller when the 5 harmonics were combined. These results correspond to oxygen determinations based on phase-shift lifetimes. Similar results are obtained for modulation-factor lifetimes (lower RMSE as more harmonics are combined) or for the combination of both (lower RMSE when modulation-factor and phase-shift lifetimes are combined).

These methods can be easily implemented in multi-frequency photoluminescence instruments since the algorithms just involve digital signal processing of the excitation and emission signals and some mathematical operations that can be computed with software.

## 6.5 Noise Analysis and Applications

As previously described, the in-phase and quadrature components of a signal at a given modulation frequency can be estimated with the I/Q method (by multiplying the signal with the corresponding cosine and sine waveforms)<sup>2,21</sup> or with the FFT.<sup>13</sup> Both methods are identical if the duration of the signal to be analyzed contains an integer number of cycles of the corresponding harmonic (otherwise the harmonic spectral power is spread around several FFT components). One advantage of the FFT analysis is that the I/Q information is obtained not only at the harmonic of interest, but also at all the

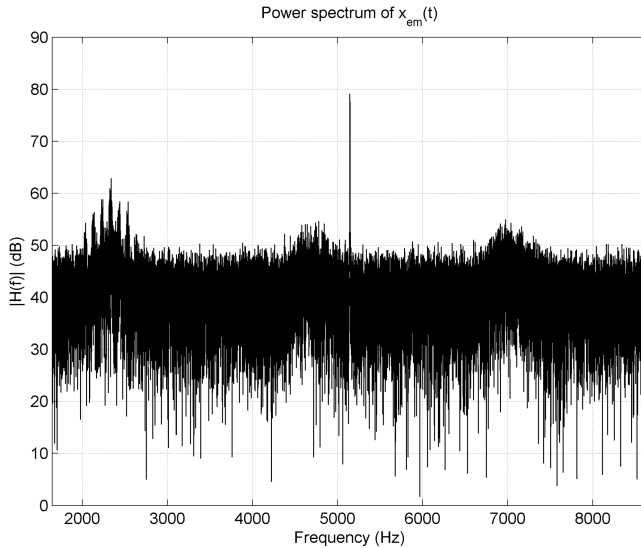


**Figure 6.5** FFT of an emission signal for sinusoidal excitation with modulation frequency  $f_0 = 5145$  Hz.

frequency components, and therefore the FFT can be applied to analyze the noise affecting the measurements. Additionally, the FFT algorithm is very efficient and computational cost is low even for relatively long signals. Figure 6.5 shows the FFT spectrum of an emission signal obtained with a sinusoidally modulated excitation. The spectral peak corresponding to the emission signal can be identified at the modulation frequency, and the FFT components in the vicinity of the modulation frequency provide information about the noise affecting this harmonic.

Using the FFT, the power spectral density of the noise (*i.e.* a statistical characterization of the noise) can be estimated around each harmonic of interest. The real and imaginary parts of the FFT components corresponding to background noise follow a Gaussian probability distribution with null mean and variance equal to the power spectral density of the noise.<sup>36</sup> Medina *et al.* proposed and evaluated an accurate method for estimating the variance (or the standard deviation) of the noise around the harmonic of interest.<sup>13</sup> This method involves an FFT computation, the selection of the frequency range used for characterizing the noise, removing outliers (corresponding to other signals or interferences but not to background noise) and estimating the standard deviation of the distribution. The method, therefore provides a characterization of the noise around the modulation frequency valid for white noise (*i.e.* if the spectral distribution of the noise is flat) or even for colored noise (for noise spectral distribution changing with the frequency).

Using the statistical characterization of the noise (*i.e.* the standard deviation of the real or imaginary parts in the FFT domain  $\sigma_N$ ), and assuming

that the modulation frequency component is affected by a noise with the same statistics, the standard error of the I/Q estimations can be easily computed:<sup>13</sup>

$$\sigma_{\text{niQ}} = \frac{2}{L} \sigma_{\text{N}} \quad (6.23)$$

where  $L$  is the number of samples in the signals to be processed  $x_c[l]$ .

### 6.5.1 Application to Uncertainty Estimation

The standard error affecting the I/Q components can be used to estimate the uncertainty of all the parameters related to the oxygen determination. It simply requires to apply the error propagation theory with the equations providing the parameters (from I/Q components to the oxygen determinations). Medina *et al.*<sup>13</sup> have applied the FFT-based noise analysis of the excitation and emission signals to estimate the uncertainty of the modulation-factor, the phase-shift, the lifetimes and the oxygen determinations. A comparison of the standard error prediction (derived from the FFT-based noise analysis) with the standard errors estimated from a collection of measurements demonstrated the utility of this method.

Even though the uncertainty estimation based on the FFT noise analysis involves some mathematical complexity, the fundamentals are simple (the uncertainty of the primary parameters can be estimated from the FFT and is then propagated to the oxygen determination) and the implementation in a computational system (a microcontroller or a computer) does not involve any difficulty.

This method allows the phosphorescence instrument to provide not only the oxygen determinations but also the corresponding standard errors (or the confidence intervals). Since the standard errors are derived from the recorded signals involved in the oxygen determination, the uncertainty estimation is specifically describing the effect of the particular measuring conditions (taking into account the amplitudes of the excitation and emission signals and the noise affecting them at the modulation frequency). This uncertainty describes the effect of the electronic noise in the excitation or the emission signal, the SNR reduction of the emission signal due to the quenching at a given oxygen concentration or due to photodegradation of the sensing phase. The uncertainty also describes the effect of the modulation frequency taking into account both, the emission intensity (that decreases with the frequency) and the spectral distribution of the noise.

The uncertainty estimation is very useful for the phosphorescence instrument. Under low illumination conditions (for example, when the phosphorescence instrument is configured to measure small samples with an optical fiber) or when the emission efficiency decreases (if the sensing dye is changed)<sup>4,12,15,19,27</sup> the operator can immediately evaluate the impact in the instrument accuracy at the current measuring conditions. Additionally, from a single measurement, the operator can determine how many times

the measurement should be repeated in order to achieve a predefined accuracy (the uncertainty decreases with the square root of the number of independent measurements). The uncertainty can be also applied to evaluate the degree of photodegradation of the sensing phase and decide when it should be replaced. It can be also used to decide when the instrument should be recalibrated (when the measurement and the confidence interval using a calibrating pattern are not statistically compatible with the calibrating value).<sup>13</sup>

### 6.5.2 Application to Optimal Combination of Harmonics

The FFT-based noise analysis provides an estimation of the standard error affecting the oxygen determination. This method can be applied to modulation-factor or to phase-shift based oxygen determinations, and can be also applied to single-frequency signals or to multi-frequency signals.

Additionally, the FFT analysis of a pair of multi-frequency signals  $x_{\text{exc}}[l]$  and  $x_{\text{em}}[l]$  provides several independent oxygen determinations (for both, modulation-factor and phase-shift based lifetimes and for different harmonics). Since a set of independent oxygen determinations, each one with its corresponding standard error, is available, different determinations can be optimally combined using eqn (6.21) in order to obtain a more accurate oxygen determination. Compared with the combination proposed in ref. 2 (where the standard errors are estimated during calibration), this combination is better adapted to the specific measuring conditions (since both, the independent oxygen determinations and the corresponding standard errors are directly estimated from the signals  $x_{\text{exc}}[l]$  and  $x_{\text{em}}[l]$ ).

The real-time combination of multi-frequency oxygen determinations using the FFT-based noise analysis has been applied with short duty-cycle rectangular signals.<sup>31</sup> Figure 6.6 shows the RMSE achieved by the phosphorescence instrument when different independent determinations are combined according to their respective standard errors. As in the case of pre-calibrated standard errors (Figure 6.4), the combination of determinations using the estimated uncertainties reduces the RMSE (lower as more harmonics are combined and lower when modulation-factor and phase-shift estimations are combined).

## 6.6 Instrument Development

Since the beginning of phase modulation phosphorescence detection, many instruments, based on different technologies and principles, have been developed.<sup>1,8,37</sup> Conventionally, most of the measurement schemes were based on sinusoidally modulated excitation sources and phase detection was performed at a single frequency with analog lock-in amplifiers<sup>12,16,23</sup> or specialized analog circuits.<sup>17,20,38</sup> Nowadays, digital technology is displacing the analog instruments, with the consequent reduction of costs and improvement of the flexibility of the modern phosphorescence instruments.

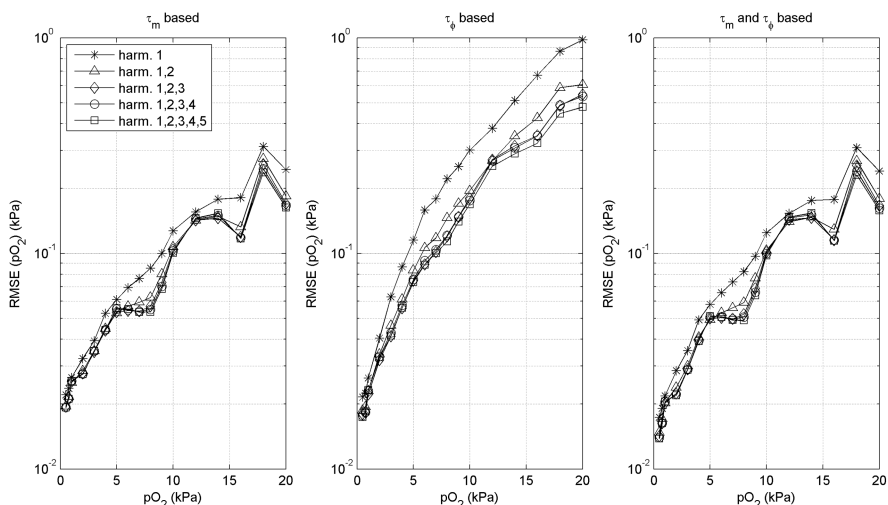


**Figure 6.6** RMSE in determination of  $pO_2$  using multi-frequency modulation (rectangular signals) and combining different harmonics. Oxygen determinations based on modulation-factor (left panel), phase-shift (center panel) and combining both (right panel). The procedure for combining the independent determinations was based on the FFT noise analysis.

The technological advances in the design and manufacturing processes of micro-computers, microcontrollers, electronic/optoelectronic components, *etc.* (with lower costs, better capabilities and smaller sizes) allow the design of modular low-cost phosphorescence instruments according to the architecture previously proposed in this chapter and incorporating the methods described in the previous sections. The proposed modular architecture allows the configuration of the excitation signal, the modulation of the illumination source, the acquisition of both the excitation and the emission signals, and digital signal processing of both signals as well as the associated mathematical computations in order to obtain the instrument response (that could be a characterization of the phosphorescent system or an oxygen determination).

In our laboratories, the experimental set-up prepared for different research purposes has been modified according to the specific requirements of each experiment. In this way, the excitation signal has been generated either with a DA board or with a microcontroller;<sup>21,27</sup> different LEDs, optical filters and sensing phases have been mounted;<sup>23–25</sup> sometimes the photodiode<sup>16</sup> has been substituted by a photomultiplier tube;<sup>2,9,21</sup> DA conversion has been performed with a digital oscilloscope or with a microcontroller,<sup>2,9,13,31</sup> *etc.* However, even though one or several elements have been changed for different experiments, the modular architecture has always been maintained, and in all the cases, the digital signal processing and the mathematical computations are applied to the digital excitation and emission signals. The advantages of all the algorithms described in this chapter just involve numerical computation with the digital signals that can be easily programmed in a computer or a microcontroller, and

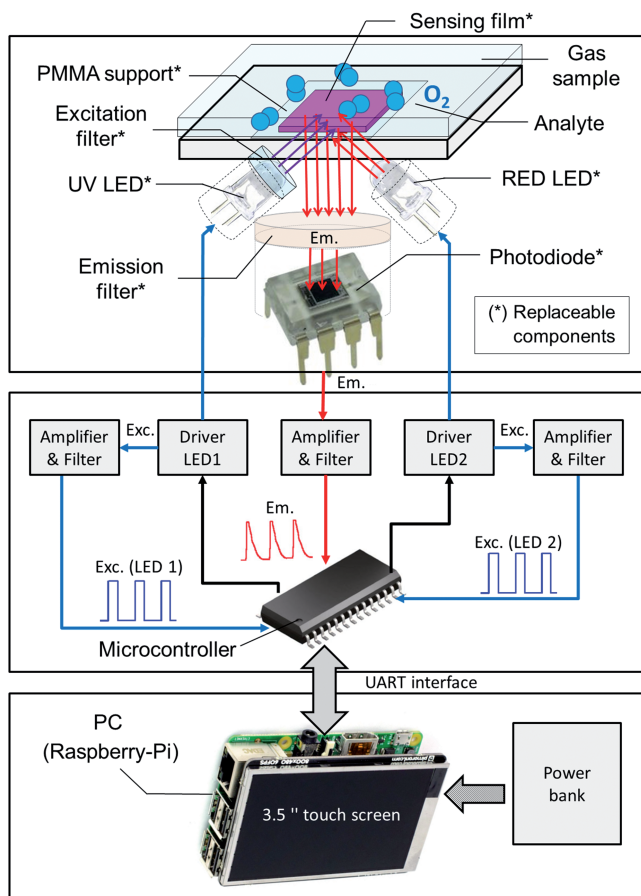


**Figure 6.7** Main components of the modular and portable phosphorescence instrument.

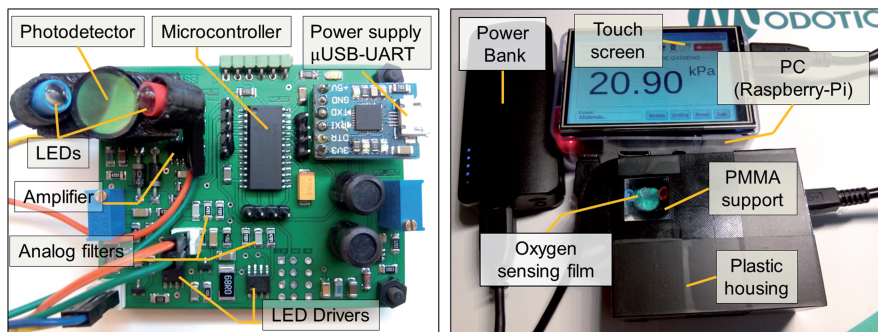
therefore the implementation of these methods does not involve significant changes in the instrument architecture or in the instrument costs.

Figure 6.7 shows a schematic diagram of the elements in a portable phosphorescence instrument for oxygen determination developed at our laboratories. The optical subsystem includes two LEDs, the photodetector, the optical filters, a support for the sensing film and the sensing film. One of the LEDs is used for exciting the sensing film (UV LED) while the other is a red LED (wavelength in the same range of the phosphorescence emission) used for calibrating the response of the photodetector (*i.e.* for measuring delay of the photodetector and the analog electronics for signal conditioning),<sup>19</sup> which is relevant for accurate characterization of the sensing film. The photodetector is a preamplifier photodiode. All these optical and optoelectronic elements are replaceable (in order to substitute degraded components or for changing the sensing dye and accommodate the new excitation and emission wavelengths).

Each LED is driven with its respective driver circuit. This circuit receives the signal used as excitation from a microcontroller and provides enough current to modulate the LED with an appropriate intensity. The LED driver also includes a circuit to provide a reference of the excitation signal. The photodiode transforms the phosphorescence response into an electrical signal. The analog signal provided by the photodiode is amplified and filtered. Both the excitation and the emission signals are AD converted and registered by the microcontroller. The microcontroller, the signal conditioning circuits and the optoelectronic and optical elements are integrated in a printed circuit board (PCB). This board also includes a UART (universal asynchronous receiver/transmitter) interface implemented with a standard micro-USB connector which allows data interchange between a computer and the board and also provides power supply.

The computer (that could be a desktop, a laptop or a micro-computer) is, in our design, a Raspberry-Pi microcomputer (with a 3.5" touch screen display). This computer configures the microcontroller for the measurements, receives the excitation and emission digital signals from the microcontroller and performs all the digital signal processing and the mathematical computations as described in this chapter in order to provide the oxygen determination (with the corresponding confidence intervals) when it is configured for oxygen measurements. It can also provide a characterization of the phosphorescent system if it is configured for this purpose. The measurements can be displayed, submitted or stored in a log file according to the system configuration. The entire instrument (including the micro-computer and the PCB) is powered with a conventional power-bank.

Figure 6.8 shows, on the left side, a picture of the printed circuit board containing the microcontroller, the UART communication module, all the specific electronics (LED drivers, filters and amplifiers), and the optical and optoelectronic elements (LEDs, optical filters, photodiode). The picture on the right



**Figure 6.8** Left panel: picture of the PCB containing the optical and electronic components of the phosphorescence instrument. Right panel: picture of the complete phosphorescence instrument including the central unit (a Raspberry- Pi PC with a touch screen display), the PCB and the power bank.

side shows the complete phosphorescence instrument including the circuit (in a plastic housing), the micro-computer Raspberry-Pi and the power bank. A compact and portable instrument has been designed ( $60 \times 85 \times 30$  mm; 180 gr). This example illustrates how the technological advances (in optoelectronics, electronics, microcontrollers and micro-computers) allow the design of flexible, modular and low-cost phosphorescence instruments incorporating advanced signal processing to optimize the acquisition of analytical information.

## 6.7 Conclusions

In this chapter we have presented the phosphorescent system from a new perspective: it can be considered as a linear system with an input (excitation) and an output (response) for which all the signal theory related to linear systems can be applied and exploited in order to optimize the performance of phosphorescence instruments. Based on this concept and bearing in mind the technological advances (better and cheaper components in the field of electronics, optics, computation, *etc.*), we have described an instrument architecture where the phosphorescent system is excited with a configurable excitation signal and where the analytical information is obtained by processing the excitation and response signals. Since both signals are digitized, all the operations required to obtain the analytical information involve digital signal processing and mathematical computation that can be implemented in a microcontroller or a computer without significant increase in the instrument cost.

In this chapter we have described some applications of signal processing, easily implementable under this architecture, with demonstrated utility for phosphorescence lifetime based oxygen sensing. Some applications are associated to the multi-frequency phosphorimetry (using multi-frequency modulated signals as excitation and applying a multifrequency processing to the excitation and emission recorded signals). This paradigm provides an easier and more complete characterization of the phosphorescent systems, it can be applied for selecting the optimal modulation frequency for oxygen determination, and it provides mechanisms for combining independent oxygen determinations (estimated for different modulation frequencies from just one multi-frequency recording) into an improved and more accurate oxygen determination. Other applications of signal processing are associated with the analysis of the background noise affecting the recorded signals. The noise characterization provides an estimation of the uncertainty affecting the oxygen determinations, which is a valuable add-on for the phosphorescence instrument. This uncertainty estimation also provides the optimal weights for combining the independent oxygen determinations obtained in multi-frequency measurements. The described procedures are easily implementable in a phosphorescence instrument designed according to the proposed architecture, as illustrated with a prototype developed at our laboratories.

The proposed architecture and the linear system perspective can be also useful for future challenges of luminescence instrumentation, such as (a) a more detailed modelling of the phosphorescent/fluorescent systems (fitting higher order differential equations, including non-linear effects in the differential equations, or including non-linear dependence of the quenching with the quencher concentration); (b) a more detailed modelling of the instrument, including a description of both the luminescent system and also the transducers; (c) an analysis of interfering quenchers and the design of multi-parametric phosphorescence instruments; or (d) adaptation of the luminescent instruments to ultra-low illumination conditions (which requires a very detailed managing of the noise in the signal processing) in order to apply them for microfluidics devices in control processes, fiber optic based sensors for small samples or micro-biosensors with optical oxygen transduction.

## Acknowledgement

This work has been partly supported by the Spanish Ministry of Economy, Industry and Competitiveness (CTQ2014-53442-P, Grant BES-2009-026919 and Torres Quevedo Grants PTQ-15-07922 and PTQ-15-07912), the CEI BioTic Granada Campus (Project CEIbioTIC14-2015) and the CEMIX UGR-MADOC-Santander Bank (Project MSOADKISS-10-2016).

## References

1. J. R. Lakowicz, *Principles of Fluorescence Spectroscopy*, Kluwer Academic, New York, 2nd edn, 1999.
2. S. Medina-Rodríguez, A. de la Torre-Vega, F. J. Sainz-Gonzalo, M. Marín-Suárez, C. Elosúa, F. J. Arregui, I. R. Matías, J. F. Fernández-Sánchez and A. Fernández-Gutiérrez, *Anal. Chem.*, 2014, **86**, 5245.
3. D. B. Papkovsky and T. C. O’Riordan, *J. Fluoresc.*, 2005, **15**, 569.
4. H. Szmecinski and J. Lakowicz, in *Topics in Fluorescence Spectroscopy*, ed. C. D. Geddes and J. R. Lakowicz, Springer, USA, 2002, vol. 4, Lifetime-based sensing, p. 295.
5. J. G. Proakis and D. G. Manolakis, *Digital Signal Processing*, Pearson Education Inc., Prentice Hall, 4th edn, 2007.
6. D. Sundararajan, *The Discrete Fourier Transform: Theory, Algorithms and Applications*, World Scientific Publishing Co. Pte. Ltd, USA, 2001.
7. R. D. Hippenstiel, *Detection Theory: Applications and Digital Signal Processing*, CRC Press, 2002.
8. O. S. Wolfbeis, *Fiber Optic Chemical Sensors and Biosensors*, CRC Press, Boca Raton, MA, 1991.
9. S. Medina-Rodríguez, A. de la Torre-Vega, C. Medina-Rodríguez, J. F. Fernández-Sánchez and A. Fernández-Gutiérrez, *Sens. Actuators, B*, 2015, **212**, 278.

10. C. M. McGraw, G. Khalil and J. B. Callis, *J. Phys. Chem. C*, 2008, **112**, 8079.
11. H. M. Rowe, S. P. Chan, J. N. Demas and B. A. DeGraff, *Anal. Chem.*, 2002, **74**, 4821.
12. M. Valledor, J. C. Campo, I. Sánchez-Barragán, J. M. Costa-Fernández, J. C. Álvarez and A. Sanz-Medel, *Sens. Actuators, B*, 2006, **113**, 249.
13. C. Medina-Rodríguez, S. Medina-Rodríguez, A. de la Torre-Vega, A. Fernández-Gutiérrez and J. F. Fernández-Sánchez, *Sens. Actuators, B*, 2016, **224**, 521.
14. C. McDonagh, C. S. Burke and B. D. MacCraith, *Chem. Rev.*, 2008, **108**, 400.
15. M. Schäferling, *Angew. Chem., Int. Ed.*, 2012, **51**, 3532.
16. O. Ergeneman, G. Chatzipirpiridis, J. Pokki, M. Marín-Suárez, G. A. Sotiriou, S. Medina-Rodríguez, J. F. Fernández-Sánchez, A. Fernández-Gutiérrez, S. Pané and B. J. Nelson, *IEEE Trans. Biomed. Eng.*, 2012, **59**, 3104.
17. G. A. Holst, T. Köster, E. Voges and D. W. Lübbers, *Sens. Actuators, B*, 1995, **29**, 231.
18. W. Trettnak, C. Kolle, F. Reininger, C. Dolezal and P. O'Leary, *Sens. Actuators, B*, 1996, **36**, 506.
19. M. Cajlakovic, A. Bizzarri, C. Konrad and H. Voraberger, *Optochemical Sensors Based on Luminescence Encyclopedia of Sensors*, American Scientific Publishers, 1st edn, 2006, vol. 7.
20. C. McDonagh, C. Kolle, A. K. McEvoy, D. L. Dowling, A. A. Cafolla, S. J. Cullen and B. D. MacCraith, *Sens. Actuators, B*, 2001, **74**, 124.
21. S. Medina-Rodríguez, A. de la Torre-Vega, J. F. Fernández-Sánchez and A. Fernández-Gutiérrez, *Sens. Actuators, B*, 2013, **176**, 1110.
22. P. Langer, R. Müller, S. Drost and T. Werner, *Sens. Actuators, B*, 2002, **82**, 1.
23. S. Medina-Rodríguez, M. Marín-Suárez, J. F. Fernández-Sánchez, A. de la Torre-Vega, E. Baranoff and A. Fernández-Gutiérrez, *Analyst*, 2013, **138**, 4607.
24. S. Medina-Rodríguez, F. J. Orriach-Fernández, C. Poole, P. Kumar, A. de la Torre-Vega, J. F. Fernández-Sánchez, E. Baranoff and A. Fernández-Gutiérrez, *Chem. Commun.*, 2015, **51**, 11401.
25. S. Medina-Rodríguez, S. A. Denisov, Y. Cudré, L. Male, M. Marín-Suárez, A. Fernández-Gutiérrez, J. F. Fernández-Sánchez, A. Tron, G. Jonusauskas, N. D. McClenaghan and E. Baranoff, *Analyst*, 2016, **141**, 3090.
26. J. N. Demas, B. A. DeGraff and W. Xu, *Anal. Chem.*, 1995, **67**, 1377.
27. S. Medina-Rodríguez, A. de la Torre-Vega, J. F. Fernández-Sánchez and A. Fernández-Gutiérrez, *Sens. Actuators, B*, 2014, **192**, 334.
28. M. Marín-Suárez, S. Medina-Rodríguez, O. Ergeneman, S. Pané, J. F. Fernández-Sánchez, B. J. Nelson and A. Fernández-Gutiérrez, *Nanoscale*, 2014, **6**, 263.
29. M. L. Meade, *Principle and Applications in Lock-in Amplifiers*, Peter Pegrins Ltd, London, 1983.
30. M. L. Mandelis, *Rev. Sci. Instrum.*, 1994, **65**, 3309.

31. S. Medina-Rodríguez, C. Medina-Rodríguez, A. de la Torre-Vega, J. C. Segura-Luna, S. Mota-Fernández and J. F. Fernández-Sánchez, *Sens. Actuators, B*, 2017, **238**, 221.
32. V. I. Ogurtsov and D. B. Papkovsky, *Sens. Actuators, B*, 1998, **51**, 377.
33. S. Lehrer, *Biochemistry*, 1971, **10**, 3254.
34. J. N. Demas and B. A. DeGraff, *Sens. Actuators, B*, 1993, **11**, 35.
35. E. R. Carraway, J. N. Demas, B. A. DeGraff and J. R. Bacon, *Anal. Chem.*, 1991, **63**, 337.
36. A. León-García, *Probability, Statistics and Random Processes for Electrical Engineering*, Pearson Education Inc., Prentice Hall, 3rd edn, 2008.
37. C. Kolle, Ph.D. Thesis, *Development and Evaluation of a Phase Fluorometric Instrumentation for Luminescence Based Optical Oxygen Sensors*, University of Leoben, July 1999.
38. G. O'Keeffe, B. D. MacCraith, A. K. McEvoy, C. M. McDonagh and J. F. McGilp, *Sens. Actuators, B*, 1995, **29**, 226.